AtMOB1 Genes Regulate Jasmonate Accumulation and Plant Development[1][OPEN]

Zhiai Guo,[a] Xiaozhen Yue,[a,b] Xiaona Cui,[a,b] Lizhen Song,[a] and Youfa Cheng[a,b,c,2,3]

[a]Key Laboratory of Plant Molecular Physiology, Institute of Botany, Chinese Academy of Sciences, Beijing 100093, China
[b]University of Chinese Academy of Sciences, Beijing 100049, China
[c]Innovative Academy of Seed Design, Chinese Academy of Sciences, Beijing 100101, China

ORCID IDs: 0000-0002-6046-4881 (Z.G.); 0000-0001-8253-9584 (Y.C.).

The MOB1 proteins are highly conserved in yeasts, animals, and plants. Previously, we showed that the Arabidopsis (*Arabidopsis thaliana*) *MOB1A* gene (*AtMOB1A/NCP1*) plays critical roles in auxin-mediated plant development. Here, we report that *AtMOB1A* and *AtMOB1B* redundantly and negatively regulate jasmonate (JA) accumulation and function in Arabidopsis development. The two *MOB1* genes exhibited similar expression patterns, and the MOB1 proteins displayed similar subcellular localizations and physically interacted in vivo. Furthermore, the *atmob1a atmob1b* (*mob1a/1b*) double mutant displayed severe developmental defects, which were much stronger than those of either single mutant. Interestingly, many JA-related genes were up-regulated in *mob1a/1b*, suggesting that AtMOB1A and AtMOB1B negatively regulate the JA pathways. *mob1a/1b* plants accumulated more JA and were hypersensitive to exogenous JA treatments. Disruption of *MYC2*, a key gene in JA signaling, in the *mob1a/1b* background partially alleviated the root defects and JA hypersensitivity observed in *mob1a/1b*. Moreover, the expression levels of the *MYC2*-repressed genes *PLT1* and *PLT2* were significantly decreased in the *mob1a/1b* double mutant. Our results showed that *MOB1A/1B* genetically interact with *SIK1* and antagonistically modulate JA-related gene expression. Taken together, our findings indicate that AtMOB1A and AtMOB1B play important roles in regulating JA accumulation and Arabidopsis development.

The Hippo signaling pathway was first described in animals. It plays pivotal roles in controlling cell proliferation, apoptosis, organ growth, and tissue homeostasis (Pan, 2010). Dysregulation of the pathway causes various cancers (Harvey et al., 2013). The core components of the pathway, including the Ste20-like kinases MST1/2, the AGC kinase NDR/LATS, and the kinase regulators MOB1 and Sav, form a kinase cascade. Sav interacts with MST1/2 and activates its kinase activity. MST1/2 phosphorylates NDR/LATS kinase and MOB1. Subsequently, MOB1 interacts with NDR/LATS and regulates kinase activity of the latter. The activated NDR/LATS in turn phosphorylates and inactivates the transcriptional coactivator YAP/TAZ (Hansen et al., 2015).

The MOB1 proteins are highly conserved from yeast (*Saccharomyces cerevisiae*) to plants and animals (Lai et al., 2005; Cui et al., 2016). The yeast *MOB1* is an essential gene required for completion of mitosis and maintenance of ploidy (Luca and Winey, 1998). In Drosophila (*Drosophila melanogaster*), disruption of *MOB1/Mats* results in increased cell proliferation, defective apoptosis, and induction of tissue overgrowth (Lai et al., 2005). In humans (*Homo sapiens*), among the 7 homologs of yeast MOB (hMOB1A, hMOB1B, hMOB2A, hMOB2B, hMOB2C, hMOB3, and hMOB4), hMOB1A and hMOB1B share more than 95% sequence identity/similarity. A biochemical characterization of hMOBs showed that only hMOB1A and hMOB1B interact with both LATS1 and LATS2 to regulate cell proliferation and apoptosis (Chow et al., 2010). In mouse (*Mus musculus*), the *mob1a/1b* double mutant showed cancer susceptibility and embryonic lethality (Nishio et al., 2012). *Mob1a/1b* double mutation in mouse liver results in the death of more than half of mutant mice within 3 weeks of birth. All survivors eventually develop liver cancers and die by age 60 weeks (Nishio et al., 2016). In addition, tamoxifen-inducible, chondrocyte-specific *Mob1a/b*-deficient mice had chondrodysplasia (Goto et al., 2018).

The Arabidopsis (*Arabidopsis thaliana*) genome contains four *MOB1* genes: *AtMOB1A*, *AtMOB1B*, *AtMOB1C*, and

[1]This work was supported by the projects from the National Natural Science Foundation of China (NSFC) (31970309; 31171389; 91217310; 91017008; 31270330), National Key Research and Development Program of China (2016YFD0100400), National Basic Research Program of China (2014CB943400), and One-hundred Talent Project of the Chinese Academy of Sciences (STS Program KFJ-STS-ZDTP-076 to Y.C.).

[2]Senior author.
[3]Author for contact: yfcheng@ibcas.ac.cn.
The author responsible for distribution of materials integral to the findings presented in this article in accordance with the policy described in the Instructions for Authors (www.plantphysiol.org) is: Youfa Cheng (yfcheng@ibcas.ac.cn).

Z.G., X.Y., X.C., and L.S. performed the experiments; Z.G. and Y.C. analyzed data and wrote the paper; Y.C. conceived and designed research.
[OPEN]Articles can be viewed without a subscription.
www.plantphysiol.org/cgi/doi/10.1104/pp.19.01434

AtMOB1D (Citterio et al., 2006; Vitulo et al., 2007; Cui et al., 2016). *AtMOB1A* is required for tissue patterning of the root tip, and sporophyte and gametophyte development (Galla et al., 2011; Pinosa et al., 2013). Recently, we reported that *AtMOB1A* plays critical roles in auxin-mediated plant development (Cui et al., 2016). The *atmob1a* mutant genetically interacts with mutants in auxin biosynthesis, signaling, and transport in many developmental processes. Interestingly, the defects of *atmob1a* can be fully rescued by the Drosophila *MOB1* gene *Mats,* suggesting conserved gene functions among different species (Cui et al., 2016). It was shown that AtMOB1A and AtMOB1B interact with SIK1, a Hippo/STE20 homolog, and regulate cell proliferation and expansion in Arabidopsis (Xiong et al., 2016). These findings demonstrate that AtMOB1A plays important roles in plant development. However, the functions of other Arabidopsis *MOB1* genes remain to be elucidated.

Jasmonates (JA) are a group of phytohormones including jasmonic acid and its derivatives. They are important in regulating plant growth and development, and plant responses to biotic and abiotic stresses. Jasmonic acid is synthesized from α-linolenic acid via the octadecanoid pathway in plastids and peroxisomes. Following synthesis, jasmonic acid is exported from the peroxisomes into the cytoplasm, where it is conjugated with Ile to produce bioactive JA-Ile. In the JA signaling pathway, JA-Ile promotes the interaction between the JA receptor COI1 and JAZ proteins. JAZ can be ubiquitinated and degraded by the 26S proteasome, leading to the release of MYC2, the major transcription factor of JA-mediated gene expression. Consequently, the JA responsive gene expression and JA responses are activated (Huang et al., 2017).

Here we show that the *mob1a/1b* double mutant displays severe developmental defects at the seedling stage. *AtMOB1B* expression was similar to that of *AtMOB1A*, and the two MOB1 proteins interacted with each other in vivo. Transcriptomic analysis indicated that the expression levels of many genes in the JA pathways were increased in the *mob1a/1b* double mutant. JA contents were also significantly increased in *mob1a/1b*. Consistently, *mob1a/1b* displayed hypersensitivity to exogenous JA treatments and the expression of *MYC2*, which encodes a key transcription factor in JA signaling, was increased. Moreover, *myc2* partially suppressed the developmental defects of *mob1a/1b*. We found that the expression levels of MYC2-repressed *PLT1* and *PLT2* in the *mob1a/1b* double mutant were significantly decreased. We conclude that AtMOB1A and AtMOB1B regulate JA accumulation, and plant growth and development.

RESULTS

AtMOB1A and *AtMOB1B* Redundantly Control Plant Development

There are four *MOB1* genes in Arabidopsis, namely *AtMOB1A*, *AtMOB1B*, *AtMOB1C*, and *AtMOB1D* (Citterio et al., 2006; Vitulo et al., 2007; Cui et al., 2016). *AtMOB1A* and *AtMOB1B* form a subgroup, whereas *AtMOB1C* and *AtMOB1D* form another clade (Fig. 1A). Previously, we reported that the loss-of-function *MOB1A* mutants, *mob1a-1* and *mob1a-2*, developed short roots and displayed small floral organs and reduced fertility compared with wild type (Cui et al., 2016).

To define functions of the other *AtMOB1* genes, we obtained transfer DNA (T-DNA) insertion mutants, denoted *mob1b-1*, *mob1c-1*, and *mob1d-1* (Fig. 1B), from the Nottingham Arabidopsis Stock Center. Reverse transcription-PCR (RT-PCR) analysis indicated that all of the mutations appeared null (Supplemental Fig. S1A). However, no obvious developmental defects were observed in the single mutants, suggesting that the *MOB1* genes may have overlapping functions. We then generated the double and triple mutant combinations (Fig. 1, C–J). Because *MOB1C* (*At5g20430*) and *MOB1D* (*At5g20440*) are located in tandem on Chromosome V, it is impossible to generate the double mutant or the quadruple mutant by genetic crossing. We thus constructed the *mob1a-2 mob1b-1 mob1c-2 mob1d-1* quadruple mutant (*mob1a-2/b-1/c-2/d-1*) using CRISPR/Cas9 gene editing technology (Gao et al., 2016; Zeng et al., 2018; Fig. 1K; Supplemental Fig. S1B) in the *mob1a-2*$^{+/-}$*/mob1b-1/mob1d-1* (*mob1a-2*$^{+/-}$*/b-1/d-1*) background.

The seedlings of *mob1a-2/b-1*$^{+/-}$ displayed smaller cotyledons, shorter roots, and a longer hypocotyl than single mutants and wild type (Fig. 1, D and E). The siliques of *mob1a-2/b-1*$^{+/-}$ adult plants were very short and completely sterile (Fig. 1, F and G). On the other hand, the *mob1a-2*$^{+/-}$*/b-1* mutant resembled *mob1b-1*. These results indicated that *AtMOB1B* became haploid insufficient in the *mob1a* mutant background. The *mob1a-2/b-1* seedlings were very tiny, and their development was significantly retarded. The 21-d-old double-mutant plants had much smaller leaves and shorter roots compared with wild type and the single mutants (Supplemental Fig. S2). To confirm that the phenotypes were caused by the mutations in *AtMOB1A* and *AtMOB1B*, we carried out genetic complementation experiments. Transformation of *mob1a-2/b-1* with the *AtMOB1A* genomic fragment resulted in plants that were similar to *mob1b-1*. We also found that *mob1a-2/b-1* plants harboring the *AtMOB1B* transgene behaved similarly to *mob1a*. Our results demonstrate that the strong developmental defects observed in the *mob1a-2/b-1* mutant are caused by the disruption of both *AtMOB1A* and *AtMOB1B* (Supplemental Fig. S3).

The *mob1a-1/b-1/c-1* and *mob1a-2/b-1/d-1* triple mutants and the *mob1a-2/b-1/c-2/d-1* quadruple mutant displayed phenotypes similar to that of *mob1a-2/b-1* (Fig. 1, H–J). Moreover, the *mob1c-2/d-1* double mutant segregated from the *mob1/a-2/b-1/c-2/d-1* quadruple mutant similar to the *mob1c-1* and *mob1d-1* single mutants and wild-type plants (Fig. 1L). These results suggest that *AtMOB1A* plays a more predominant role than *AtMOB1B*. *AtMOB1A* and *AtMOB1B* appear to be more important in regulating plant development than *AtMOB1C* and *AtMOB1D* under our growth conditions. We

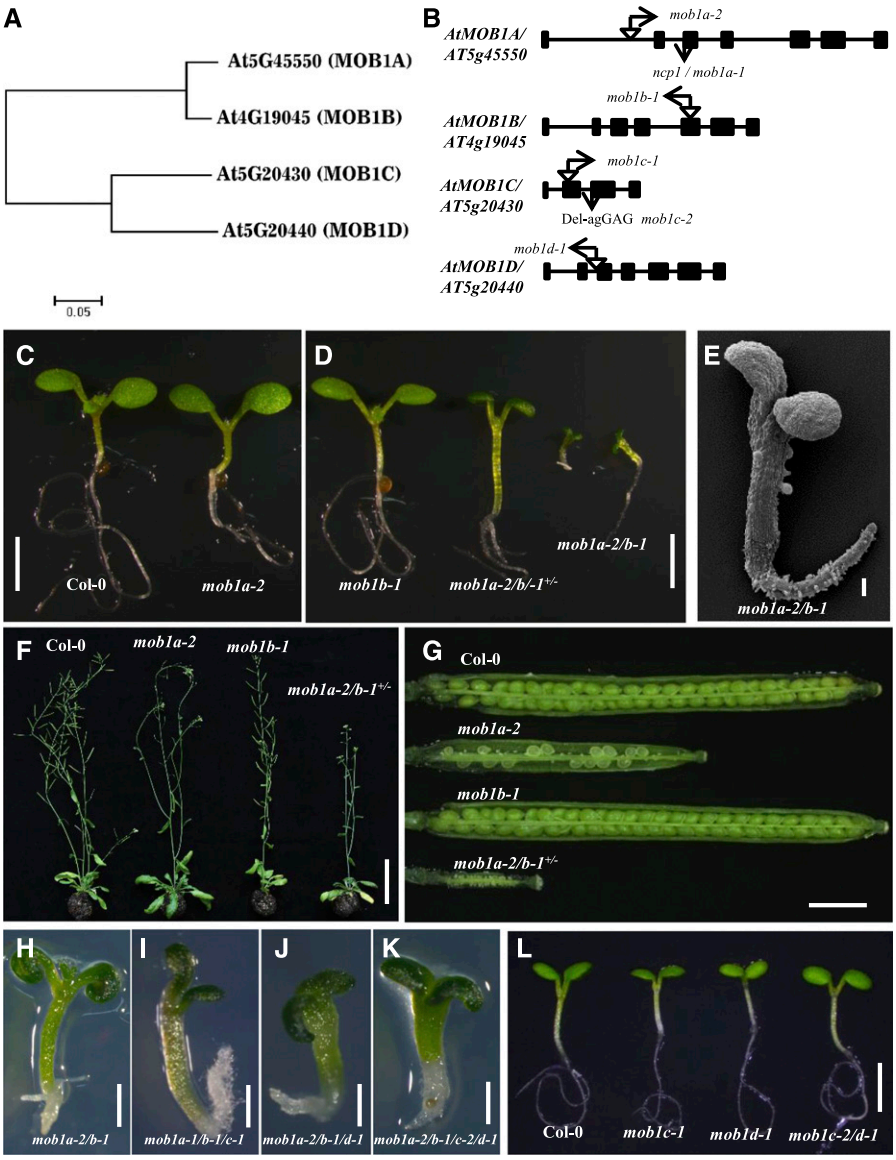

Figure 1. Analysis of loss-of-function *atmob1*mutants. A, A phylogenetic tree of AtMOB1 family proteins. B, Schematic representation of *AtMOB1* gene structures and positions of the T-DNA insertion. The 5-bp deletion in *mob1c-2* mutant was designated as "Del-agGAG" in *AtMOB1C*. C and D, 6-d-old seedlings of Col-0, *mob1a-2*, *mob1b-1*, *mob1a-2/b-1*$^{+/-}$, and *mob1a-2/b-1* mutants. E, Electron micrograph of a *mob1a-2/b-1* double-mutant seedling. F and G, Adult plants (F) and siliques (G) of Col-0, *mob1a-2*, *mob1b-1*, and *mob1a-2/b-1*$^{+/-}$. H to K, 6-d-old seedlings of *mob1a-2/b-1* (H), *mob1a-2/b-1/c-1* (I), *mob1a-2/b-1/d-1* (J), and *mob1a-2/b-1/c-2/d-1* (K). L, 6-d-old seedlings of Col-0, *mob1c-1*, *mob1d-1*, and *mob1c-2/d-1*. Scale bars = 5 mm (C and D) and 100 μm (E and H–K).

therefore focused on *AtMOB1A* and *AtMOB1B* in this work.

AtMOB1A and *AtMOB1B* Show Similar Expression Patterns

To investigate the expression patterns of *AtMOB1A* and *AtMOB1B*, we made constructs containing *AtMOB1A* or *AtMOB1B* genomic DNA sequences fused with the *GUS* gene, which were then expressed in wild-type plants. *AtMOB1A-GUS* and *AtMOB1B-GUS* were expressed with very similar patterns in cotyledons, true leaves, trichomes, root hairs, primary and lateral roots of seedlings, and floral organs (Supplemental Fig. S4, A–F and H–M).

We also generated transgenic plants containing *AtMOB1B* genomic DNA sequence fused with the *GFP* gene. AtMOB1B-GFP was expressed in the roots, and the fusion protein was localized to the nucleus, cytoplasm, and plasma membrane, similar to AtMOB1A-GFP (Supplemental Fig. S4, G and N). The subcellular localization of AtMOB1B-GFP was similar to that of AtMOB1A-GFP (Cui et al., 2016). These results are consistent with our hypothesis that *AtMOB1A* and *AtMOB1B* redundantly regulate plant development.

AtMOB1A and *AtMOB1B* Are Necessary for Cell Proliferation

The seedlings of the *mob1a-2/b-1* mutant had very short roots. The lengths of the root elongation zone and the meristem zone were dramatically decreased in the *mob1a-2/b-1* mutant (Fig. 2, A–C). The cell numbers of the elongation zone and the meristem zone were also significantly reduced in the double mutant (Fig. 2, D and E). Moreover, the root cap columella of *mob1a-2/b-1* was

much smaller (Fig. 2, F and G). These results suggest that cell division activities are abnormal in *mob1a-2/b-1*. To test this hypothesis, we used *CYCB1;1:GUS*, which is a widely used marker for the G2/M phase of the cell cycle (Colón-Carmona et al., 1999). We introduced this marker into the *mob1a-2/b-1* double and single mutant backgrounds by genetic crossing. The expression of *CYCB1;1:GUS* was decreased significantly in *mob1a-2* and slightly in *mob1b-1* single mutants, and was barely detectable in the *mob1a-2/b-1* double mutant (Fig. 2, H and I). These results suggest that both *MOB1A* and *MOB1B* are important for cell proliferation in Arabidopsis roots.

AtMOB1A Physically Interacts with AtMOB1B

We tested whether AtMOB1A and AtMOB1B physically interact with each other. We carried out an coimmunoprecipitation (Co-IP) assay in *Nicotiana benthamiana* leaves, which were cotransformed with yellow fluorescent protein (YFP)-tagged AtMOB1B and FLAG-tagged AtMOB1A. The proteins were immuno-precipitated using anti-GFP beads and detected with FLAG antibody. Our results clearly indicated that AtMOB1A and AtMOB1B physically interact in *N. benthamiana* leaves (Fig. 3A).

We also performed immunoprecipitation mass spectrometry (IP-MS) experiments using Arabidopsis seedlings transformed with *35S::AtMOB1A-FLAG*. Total protein was extracted from seedlings and immunoprecipitated with anti-FLAG antibody beads. The candidate interacting proteins were then identified by mass spectrometry. A total of 11 AtMOB1A/B peptide sequences were detected as AtMOB1A-interacting proteins. Although nine of these were shared by AtMOB1A/B, the other two were AtMOB1B specific (Supplemental Table S1), indicating that AtMOB1A and AtMOB1B interacted in the IP-MS assay in Arabidopsis.

To further confirm the interaction, we carried out the firefly luciferase complementation imaging (LCI) assay (Chen et al., 2008). The results indicated that AtMOB1A directly interacts with AtMOB1B in *N. benthamiana* leaves (Fig. 3B). Combined, these experiments show that AtMOB1A interacts with AtMOB1B in vivo.

AtMOB1A and *AtMOB1B* Negatively Regulate the JA Pathways

To identify differentially expressed genes (DEGs) between the *mob1a-2/b-1* mutant and wild type, we performed RNA-sequencing (RNA-seq) analysis using 10-d-old seedlings of *mob1a-2/b-1* and Col-0, with three biological repeats included of each genotype. A total of 1202 DEGs were identified, including 725 up-regulated and 477 down-regulated genes (Supplemental Table S2). Gene Ontology (GO) analysis revealed that many genes in the JA biosynthetic, metabolic, and signaling pathways were significantly enriched (Fig. 4A). In addition, genes involved in several JA-related biological processes were also enriched, including glucosinolate biosynthetic and metabolic processes, and responses to insects and wounding (Huang et al., 2017; Wasternack and Song, 2017; Fig. 4A; Supplemental Table S3).

We identified 89 JA-related DEGs in *mob1a-2/b-1*, which include 83 up-regulated and 6 down-regulated genes (Supplemental Table S4). First, the expression of many pivotal genes in JA biosynthesis, including the four *13-LOXs*, *AOS*, *AOC*, *OPR3*, and *OPCL* were dramatically up-regulated (Fig. 4B). Second, *JAR1*, *ILL6*, *IAR3*, *ST2A*, *JOX*, *CYP94B3*, and *CYP94C1* were also up-regulated, which encode enzymes that catalyze a number of key metabolic processes of JA and JA-Ile, including hydrolysis, sulfation, hydroxylation, and carboxylation (Fig. 4C). Third, five *JAZs* and *MYC2* in the JA signaling pathway were markedly up-regulated (Fig. 4D). Moreover, some genes involved in response to JA, such as *VSP2*, *TAT3*, and *JR2*, were also up-regulated (Fig. 4D; Supplemental Table S4).

To validate the RNA-seq results, we carried out RT-quantitative PCR (qPCR) analysis. The results confirmed the increased expression of the up-regulated DEGs in *mob1a-2/b-1* compared with that in the single mutants and wild type (Fig. 4, E–G). Therefore, AtMOB1A and AtMOB1B likely negatively regulate JA biosynthetic, metabolic, and signaling pathways.

JA Content Is Significantly Increased in the *mob1a-2/b-1* Double Mutant

The up-regulation of many genes involved in JA biosynthesis, metabolism, and signaling in the *mob1a-2/b-1* double mutant may lead to an alteration of JA concentrations. To test this hypothesis, we measured endogenous JA contents using the gas chromatography-mass spectrometry (GC-MS) method. Indeed, JA content in the *mob1a-2/b-1* mutant was dramatically increased compared with that in the single mutants and wild-type plants. JA content was similar in the single mutants and wild type (Fig. 5A). These results suggest that AtMOB1A and AtMOB1B negatively regulate JA accumulation.

The *mob1a-2/b-1* Double Mutant Is Hypersensitive to Exogenous Me-JA Treatment

It is known that JA can promote leaf senescence (He et al., 2002; Xiao et al., 2004; Shan et al., 2011). We tested whether the *mob1* single and double mutants responded to exogenous JA treatments differently than wild type. The 5-d-old seedlings of wild type, *mob1a-2*, and *mob1b-1* single mutants, and the *mob1a-2/b-1* double mutant were transferred onto half-strength Murashige and Skoog plates containing different concentration (0, 10, 25, 50, 100, and 200 μM) of Me-JA and grown for a further 14 d. The leaves of the double mutant became senescent and yellow when treated with Me-JA at 100 μM and 200 μM, whereas the wild type and the

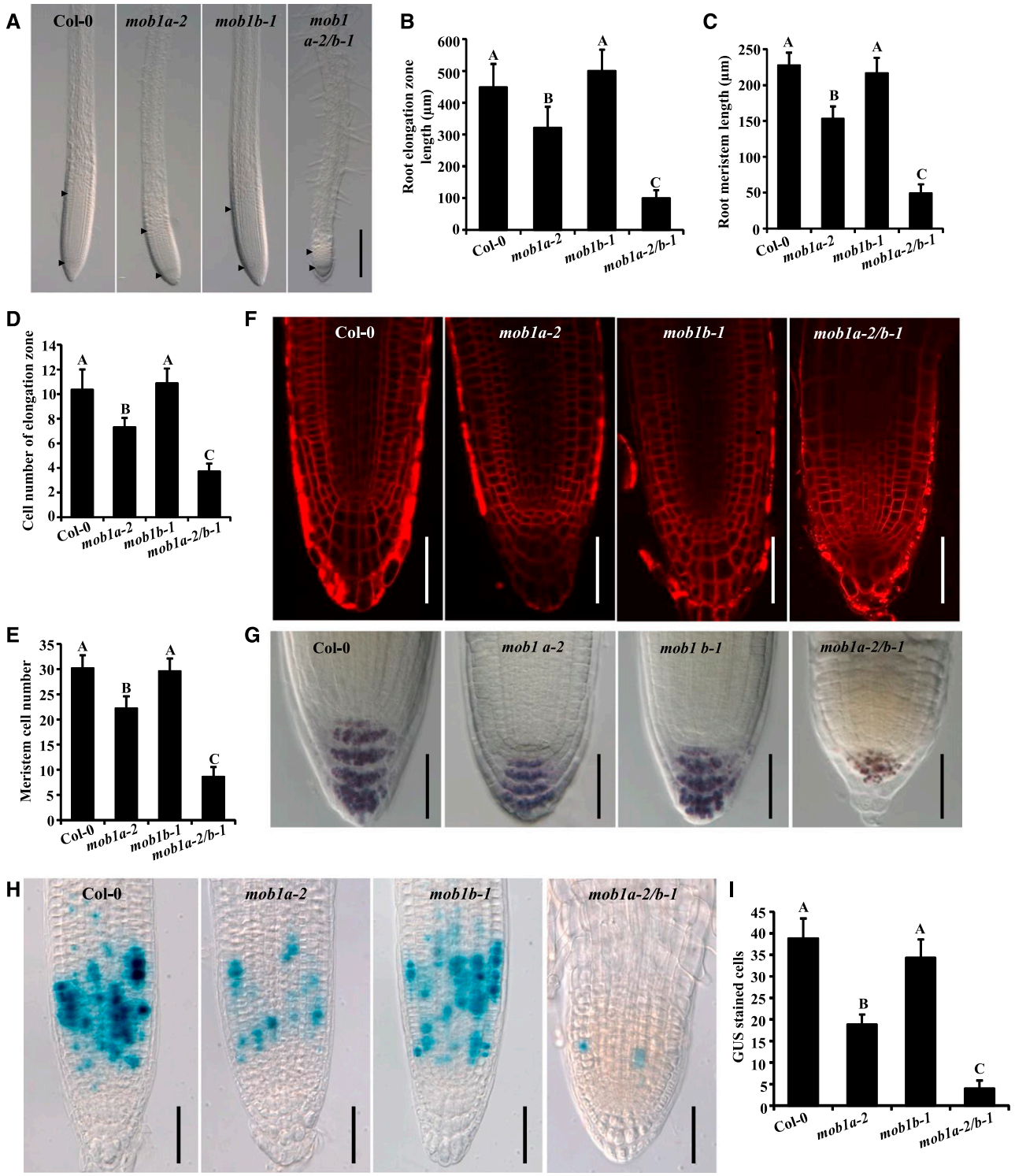

Figure 2. The *mob1a-2 b-1* mutant displays strong defects in root tips. A, The root tips of 6-d-old seedlings of Col-0, *mob1a-2*, *mob1b-1*, and *mob1a-2/b-1* mutants are shown. The meristem zone is marked with two arrowheads. B to E, Measurements of the lengths of root elongation zone (B) and meristem (C), and cell numbers in elongation zone (D) and meristem (E). F, Root tips of 6-d-old seedlings stained with FM4-64. G, The columella root cap cell of 6-d-old seedlings revealed by Lugol staining. H, *CYCB1;1:GUS* expression in the root of 6-d-old seedlings. I, Quantification of cells with *CYCB1;1:GUS* signal in (H). Data represent means ± SD. Different letters represent the significance at the $P < 0.001$ level (one-way ANOVA, LSD test); $n > 20$. Scale bars = 200 μm (A) and 50 μm (F–H).

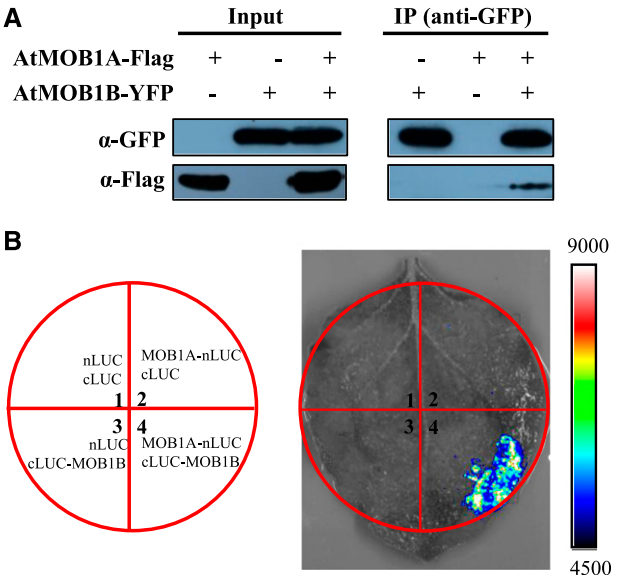

Figure 3. Physical interaction between AtMOB1A and AtMOB1B proteins in vivo. A, Co-IP assay of AtMOB1A and AtMOB1B. AtMOB1B-GFP was immunoprecipitated by using anti-GFP agarose beads, followed by immunoblot with anti-Flag antibody, and AtMOB1A-Flag was detected. B, LCI assays showing the interaction between MOB1A and MOB1B in *N. benthamiana* leaf cells. Left shows the combinations of agrobacteria containing the indicated plasmids used to coinfiltrate into different leaf regions shown at right. Empty cLUC and nLUC vectors were used as negative controls. The experiments were carried out with three independent biological repeats.

single mutants remained green (Supplemental Fig. S5). In addition, RNA-seq results indicated that several senescence-associated genes displayed altered expression in the double mutant (Supplemental Table S5), including up-regulated *Senescence-associated gene 21* (*SAG21*/AT4G02380), *Senescence/dehydration-associated protein-related A*/(AT4G15450), and *ERD7/Senescence/dehydration-associated protein-related* (AT2G17840), and down-regulated *Rubisco Activase* (*RCA*), and *Senescence-associated family protein* (AT1G66330). These results are consistent with the observed increase in JA content in the double mutant.

Disruption of *MYC2* Partially Rescues the Developmental Defects and JA Hypersensitivity of *mob1a-2/b-1*

The increased expression of JA-related genes and JA content in the *mob1a-2/b-1* double mutant suggested that *AtMOB1A* and *AtMOB1B* negatively regulate JA accumulation. To test the biological relevance of these observations, we analyzed the genetic interaction between *myc2-2* and the *mob1a-2/b-1* double mutant. *MYC2* encodes a key downstream transcription factor that regulates diverse aspects of JA responses, and its expression was also found to be up-regulated in *mob1a-2/b-1* (Supplemental Table S4; Fig. 4G). We introduced the *myc2-2* mutation into the *mob1a-2/b-1* background by genetic crossing. The *myc2-2 mob1a-2/b-1* triple mutant developed longer roots than the *mob1a-2/b-1* double mutant (Fig. 5, B–D), indicating that the *myc2-2* mutation can partially suppress the root defects of *mob1a-2/b-1*.

Because *MYC2* plays critical roles in activating JA-induced leaf senescence (Qi et al., 2015), we examined JA-induced senescence in the *myc2-2 mob1a-2/b-1* triple mutant. It was clear that the *myc2-2* mutation repressed the JA hypersensitivity of the *mob1a-2/b-1* double mutant. Both the morphological defects and decreased chlorophyll content of *mob1a-2/b-1* were suppressed by *myc2-2*. (Fig. 5, E and F). These results suggest that the root defects and JA hypersensitivity of the *mob1a-2/b-1* double mutant are partially caused by overaccumulation of JA, and are dependent on *MYC2*-mediated JA signaling.

Expression Levels of *PLT1* and *PLT2* Are Decreased in the *mob1a-2/b-1* Double Mutant

PLETHORA (PLT) 1 and *PLT2* encode proteins belonging to the AP2 class of transcription factors, and are essential for root stem cell niche patterning (Aida et al., 2004; Galinha et al., 2007). It is known that MYC2 represses the expression of *PLT1* and *PLT2*, which restricts root meristem activity and inhibits primary root growth (Chen et al., 2011). To investigate the expression of *PLT1* and *PLT2* in *mob1a-2/b-1*, we introduced markers *pPLT1:cyan fluorescent protein* (*pPLT1:CFP*) and *pPLT2:CFP* (Galinha et al., 2007) into the mutant backgrounds by genetic crossing. The expression levels of *pPLT1:CFP* and *pPLT2:CFP* were significantly decreased in the *mob1a-2/b-1* double mutant compared with that in the single mutants and wild type (Fig. 6, A–D). We further introduced the *pPLT1:PLT-YFP* and *pPLT2:PLT-YFP* fusions (Galinha et al., 2007) into the mutant backgrounds by genetic crossing, and found that, in agreement, the resulting protein levels were also significantly decreased in *mob1a-2/b-1* compared with that in the single mutants and wild type (Fig. 6, E–H). To examine the root stem cell identity, we introduced the quiescent center marker *pWOX5::GFP* into the mutant backgrounds by genetic crossing. The GFP signals were detected in the quiescent center cells (Supplemental Fig. S6), indicating that the root stem cell identity was still maintained. These results suggest that up-regulated *MYC2* expression represses *PLT1/2* expression in the *mob1a-2/b-1* double mutant, which at least partially accounts for the root developmental defects.

Genetic Interaction Between *mob1a-2/b-1* and *sik1* Mutants

It was previously reported that the Hippo/STE20 homolog SIK1 interacts with MOB1 to regulate cell proliferation and cell expansion in Arabidopsis (Xiong et al., 2016). *sik1* mutant plants are smaller than wild type (Xiong et al., 2016), and the JA levels in the *sik1* mutant are decreased compared with wild type (Zhang

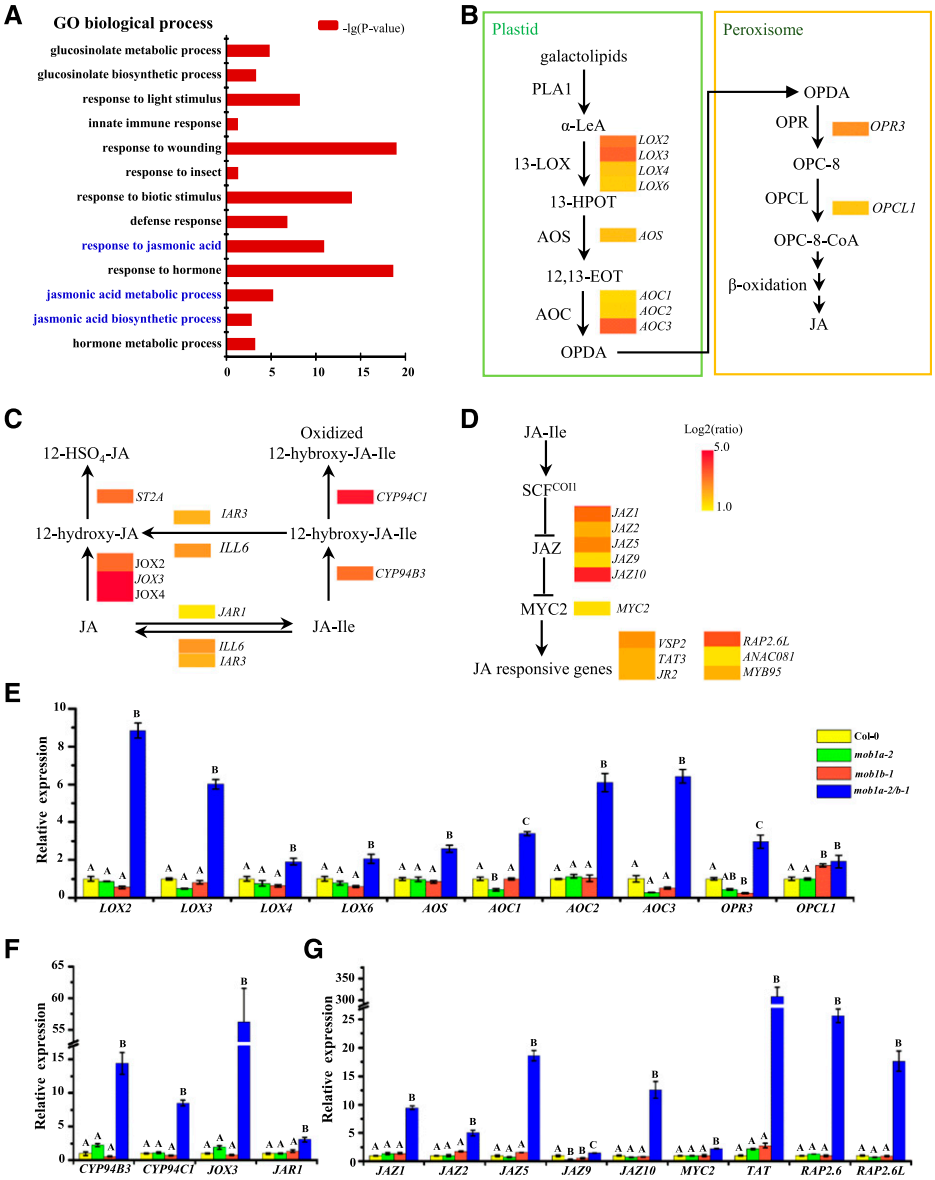

Figure 4. Expression of genes involved in JA biosynthesis, metabolism, and signaling are altered in the *mob1a-2/b-1* double mutant. A, Functional assignment of the DEGs by GO enrichment analysis. Bars = –lg (P value), and the P values were adjusted by the Bonferroni approach. B to D, DEGs in jasmonic acid biosynthesis (B), metabolic processes of JA and JA-Ile (C), and JA signaling pathway and response to JA (D). The heatmap indicates the ratio being up-regulated. Scale colors represent log2(ratio). α-LeA, α-linolenic acid; 13-HPOT, 13-hydroperoxylinoleic acid; 12,13-EOT, 12,13-epoxyoctadecatrienoic acid; OPDA, 12-oxophytodienoic acid; OPC-8, 3-oxo-2-(2-pentenyl)-cyclopentane-1-octanoic acid; PLA1, phospholipase A1; 13-LOX, 13-lipoxygenase; AOS, allene oxide synthase; AOC, allene oxide cyclase; OPR, OPDA reductase; OPCL, OPC-8-CoA ligase; ST2A, 12-OH-JA sulfotransferase; JOX, jasmonic acid oxidase; JAR1, jasmonoyl Ile syntase; ILL6 and IAR3, IAA-amino acid hydrolase; CYP94C1; 12-OH-JA-Ile carboxylase; JAZ, jasmonate-zim-domain protein; MYC2, bHLH zip transcription factor; VSP2, vegetative storage protein 2; TAT3, Tyr aminotransferase 3; JR2, jasmonic acid responsive 2; RAP2.6L, ERF/AP2 transcription factor; ANAC081, Arabidopsis NAC domain containing protein 81. E to G, Relative expression of the DEGs in JA biosynthesis (E), metabolism (F), and signaling (G) in Col-0, *mob1a-2, mob1b-1*, and *mob1a-2/b-1*. Ten-day-old seedlings were collected for RNA extraction and RT-qPCR analysis. *ACTIN2* was used as an internal control. The expression levels of the indicated genes in Col-0 were set to 1. Error bars = SD of three biological repeats. Different letters indicate significant difference at $P < 0.001$ (one-way ANOVA, Tukey post-test).

et al., 2018). We generated a *sik1 mob1a-2/b-1* triple mutant by genetic crossing, and found that seedlings of the resulting triple mutant were smaller than *mob1a-2/b-1* double-mutant seedlings (Fig. 7, A–C). Because JA levels are increased in *mob1a-2/b-1* but decreased in *sik1* mutant, we examined the expression of several JA-responsive genes in these mutant backgrounds. The expression levels of *JAZ1*, *JAZ2*, *JAZ5*, *JAZ9*, *JAZ10*,

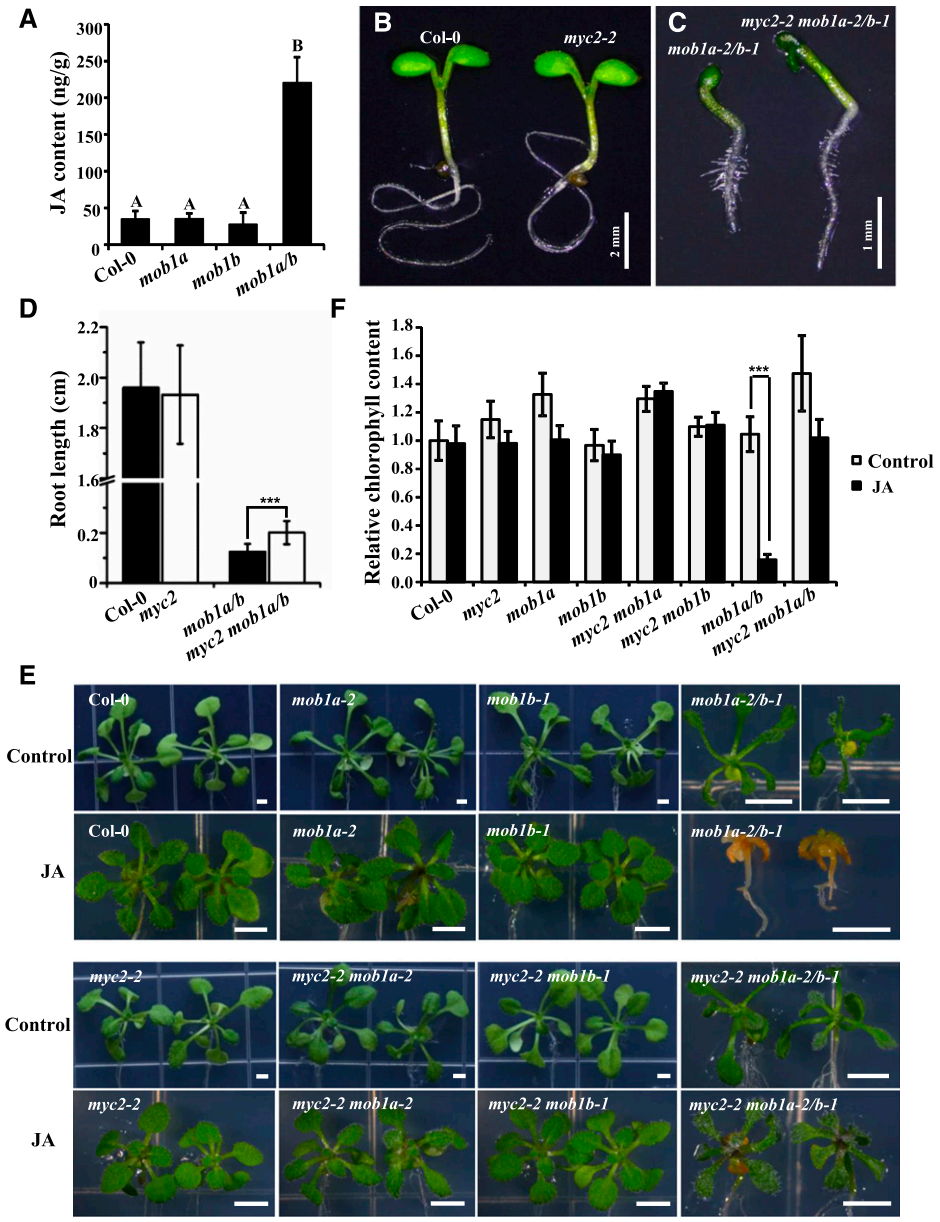

Figure 5. AtMOB1A and AtMOB1B negatively regulate JA accumulation. A, Measurement of the JA contents in seedlings of Col-0, *mob1a-2*, *mob1b-1*, and *mob1-2/b-1* mutants by using GC-MS. Seedlings were grown on half-strength Murashige and Skoog medium for 14 d after germination. Data represent means ± SD of three independent biological repeats. Different letters represent statistical significance at the $P < 0.001$ level (one-way ANOVA, LSD test). B and C, 6-d-old seedlings of Col-0, *myc2-2*, *mob1a-2/b-1*, and *myc2-2 mob1a-2/b-1* mutants. Seedlings were grown on half-strength Murashige and Skoog medium for 6 d after germination. Scale bars = 2 mm (B) and 1 mm (C). D, Measurement of root length of Col-0, *myc2-2*, *mob1a-2/b-1*, and *myc2-2 mob1a-2/b-1* mutants. Data represent means ± SD ($n \geq 20$) with significant differences determined by Student's *t* test. ***$P < 0.001$ compared with *mob1-2 b-1*. E, *mob1a-2/b-1* mutants were hypersensitive to exogenous JA treatment. Five-day-old seedlings grown on half-strength Murashige and Skoog plates were transferred to the half-strength Murashige and Skoog plates without (Control, top) or with (JA, bottom) 100 μM Me-JA and grown for 2 weeks. Scale bars = 2 mm. F, Measurement of chlorophyll contents. The chlorophyll contents of indicated mutants are relative to that in Col-0, which was set to 1.0. Data represent means ± SD ($n = 15$). Student's *t* test. ***$P < 0.001$ compared with control.

and *MYC2* were increased in *mob1a-2/b-1* but significantly decreased in the *sik1* mutant. The expression levels of these genes were increased in the *sik1 mob1a-2/b-1* triple mutant compared with in the *sik1* mutant (Fig. 7D). These results suggest that changes to JA-responsive gene expression caused by the *mob1a-2/b-1* mutations were partially alleviated by the *sik1* mutation in the *sik1 mob1a-2/b-1* triple mutant, consistent with the observed differences in JA levels in *mob1a-2/b-1* and *sik1*.

DISCUSSION

In this paper, we report that *AtMOB1A* and *AtMOB1B* genetically and physically interact to control Arabidopsis development. The *mob1a-2/b-1* double mutant was reduced in size with severe developmental defects, and the expression levels of many genes in the JA biosynthetic, metabolic, signaling, and responses pathways were up-regulated. Consistent with these observations, *mob1a-2/b-1* accumulated much more JA than the single mutants and wild type, and the double mutant was hypersensitive to JA treatment. Disruption of the key JA signaling gene *MYC2* partially alleviated *mob1a-2/b-1* root defects and JA hypersensitivity. *mob1a-2/b-1* was associated with decreased expression of *PLT1/2*, suggesting that altered expression of these critical root development genes partially accounts for the observed root defects.

AtMOB1A and AtMOB1B Interact to Regulate Growth and Development

Previously, it has been shown that AtMOB1A is important for many plant development processes (Citterio

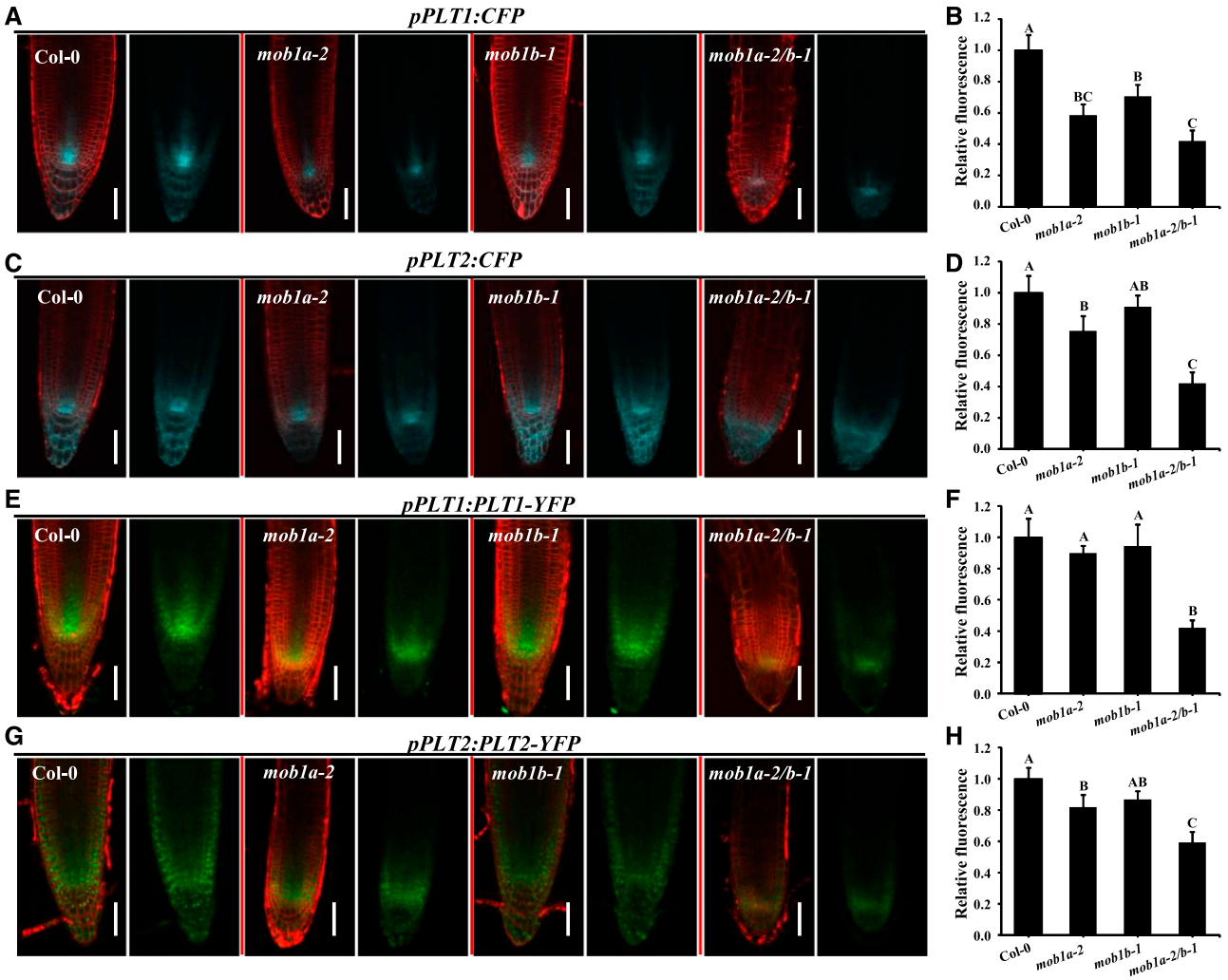

Figure 6. Expression levels of *PLT1* and *PLT2* are reduced in *mob1a-2/b-1*. A, C, E, and G, Representative expression of *PLT1:CFP* (A), *PLT2:CFP* (C), *PLT1:PLT1-YFP* (E), and *PLT2:PLT2-YFP* (G) in the root tips of 6-d-old Col-0, *mob1a -2*, *mob1b-1*, and *mob1a-2/b-1* mutant seedlings. Scale bars = 50 μm. B, D, F, and H, Quantification of CFP (A, C) and YFP (E, G) fluorescence, respectively. The fluorescence strength of Col-0 was set to 1. Data represent means ± SD (n = 15). Different letters represent statistical significance at the $P < 0.001$ level (one-way ANOVA, LSD test).

et al., 2006; Pinosa et al., 2013; Cui et al., 2016) and that AtMOB1A plays critical roles in auxin-mediated development (Cui et al., 2016). Although the *mob1a* single mutant plants displayed strong developmental defects and the *mob1b* phenotype was similar to wild type, *mob1a-2/b-1* showed an enhanced mutant phenotype compared with *mob1a-2* and *mob1b-1*, indicating that *AtMOB1A* and *AtMOB1B* have unique and overlapping functions. Interestingly, such genetic interaction and redundant or overlapping function of MOB1A/B were also observed in mouse. The mouse *mob1a/b* double mutant exhibited embryonic lethality or severe cancer susceptibility (Nishio et al., 2012). *Mob1a/1b* double mutation in mouse liver resulted in death within 3 weeks of birth or liver cancers and death by age 60 weeks (Nishio et al., 2016).

On the other hand, AtMOB1A and AtMOB1B proteins physically interact in vivo. The interaction between hMOB1A and hMOB1B was also reported in humans (Wang et al., 2014), suggesting that the interaction between these two proteins is also conserved. Previously, it was reported that Arabidopsis Ser/Thr kinase 1 (SIK1) is a Hippo homolog and that AtMOB1A and AtMOB1B interact with SIK1 (Xiong et al., 2016). These genetic and physical interactions suggest that SIK1, AtMOB1A, and AtMOB1B form a large protein complex. Interestingly, the *sik1 mob1a-2/b-1* triple mutant displayed stronger developmental defects compared with the *mob1a-2/b-1* double mutant, suggesting that there might be additional components involved in regulating the affected developmental processes. There are 10 *SIK1*-like genes in the MAP4 Kinase family (Zhang et al., 2018). It is possible that other members of the MAP4 family play redundant roles with SIK1. Recently, it was shown that SIK1 associates with, phosphorylates, and stabilizes the

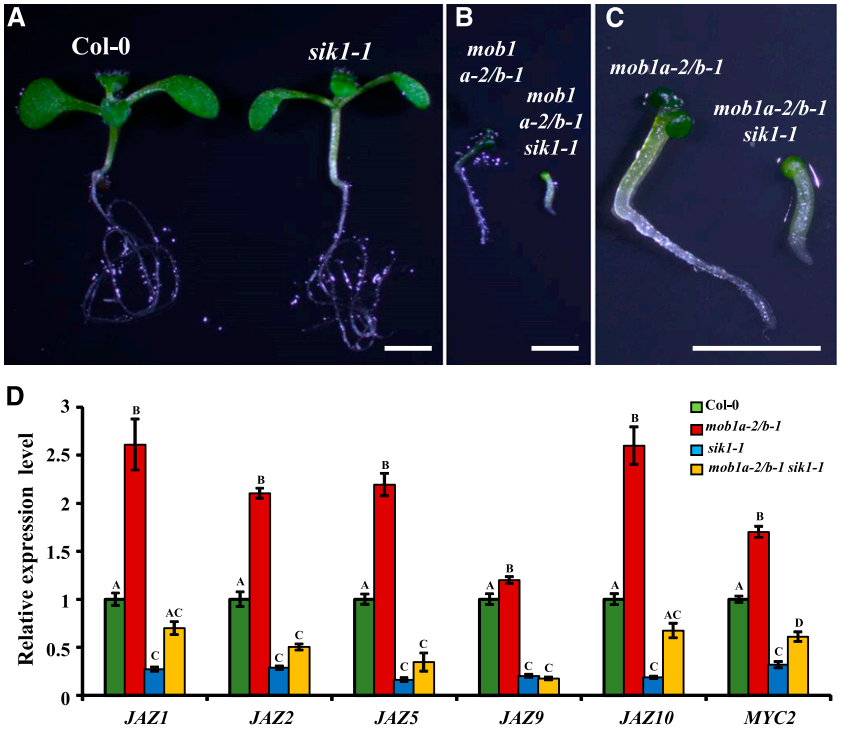

Figure 7. Genetic interaction between *MOB1A/B* and *SIK1*. A and B, 12-d-old seedlings of Col-0, *sik1-1*, *mob1a-2/b-1*, and *mob1a-2/b-1 sik1-1* mutants. C, Close-up of seedlings in (B). Note the triple mutant was smaller than the double mutant. Scale bars = 2 mm. D, Relative expression of JA signaling-related genes in 12-d-old seedlings of Col-0, *mob1a-2/b-1*, *sik1-1*, and *mob1a-2/b-1 sik1-1*. *ACTIN2* was used as an internal control. The expression levels of the indicated genes in Col-0 were set to 1. Different letters indicate significant difference at $P < 0.001$ ($n = 3$, one-way ANOVA, Tukey post-test).

central immune regulator BIK1 (Zhang et al., 2018). On the other hand, MOB1s are adaptor/scaffolding proteins. It is not clear whether SIK1 phosphorylates MOB1 and/or MOB1 activates SIK1 kinase activity.

Because the phenotypes of the *mob1a-2/b-1* double mutant are stronger than those of the *mob1a-2* and *mob1b-1* single mutants, it is likely that AtMOB1B and AtMOB1A proteins also form homodimer/oligomers. Also, because the *mob1a-2* mutant displayed strong developmental defects, whereas *mob1b-1* was largely normal, it is likely that AtMOB1A plays the dominant role. Indeed, a total of 11 AtMOB1A/B peptide sequences were detected as AtMOB1A-interacting proteins. Nine of these were shared by AtMOB1A/B, and the remaining two were AtMOB1B specific (Supplemental Table S1). These results indicate AtMOB1A and AtMOB1B interacted in the IP-MS assay in Arabidopsis, and further suggest that AtMOB1A and AtMOB1B form homodimer/oligomers.

AtMOB1A and AtMOB1B Modulate JA Accumulation

JAs are important in regulating plant growth and development as well as plant responses to biotic and abiotic stresses. JA inhibits primary root growth and promotes leaf senescence (Huang et al., 2017). We found that *mob1a-2/b-1* mutant plants had a very small growth habit, with small cotyledons and short roots. It was reported that JA treatment markedly reduces the expression of *CYCB1;1:GUS* and represses cell division activity in Arabidopsis root meristems (Chen et al., 2011). We showed that the expression of *CYCB1;1:GUS* was dramatically decreased in *mob1a-2/b-1* mutant plants (Fig. 2), which is consistent with their higher JA level (Fig. 5). These results suggest that the short root phenotype of the *mob1a-2/b-1* double mutant could be partially caused by JA-induced repression of root cell division.

The expression levels of many genes involved in JA biosynthetic, metabolic, and signaling pathways were increased, and JA content was elevated in *mob1a-2/b-1*. Moreover, the expression of *MYC2* was increased and the expression of *PLT1/2* was decreased in the double-mutant plants. These observations are consistent with the findings that JA reduces the expression levels of *PLT1* and *PLT2*, which is mediated by the direct binding of MYC2 to the promoters of *PLT1* and *PLT2* to repress their expression (Chen et al., 2011). Moreover, disruption of *MYC2* in the *mob1a-2/b-1* background partially alleviated the short-root phenotype, suggesting that the root defects were at least partially caused by increased endogenous JA. The *mob1a-2/b-1* double mutant was hypersensitive to exogenous Me-JA treatment in terms of leaf senescence. JA-repressed *RCA*, which plays an important role in JA-induced leaf senescence (Shan et al., 2011), was among the few down-regulated DEGs in *mob1a-2/b-1* plants. Our RNA-seq analysis also revealed that expression of some JA responsive genes was altered in the *mob1a-2/b-1* double mutant, such as the up-regulation of *VPS2*, *TAT*, and *LOX3*, the most prominent marker genes responding to wounding activated by *MYC2* in the JA signaling pathway (Titarenko et al., 1997; Lorenzo et al., 2004). More importantly, the JA hypersensitivity of the *mob1a-2/b-1* double mutant was markedly alleviated by the

myc2 mutation in *myc2-2 mob1a-2/b-1* plants. These results suggest that the elevated JA content in the *mob1a-2/b-1* double mutant caused the JA-related phenotypes. Intriguingly, disruption of *MYC2* only mildly suppressed the extreme short-root phenotype observed in *mob1a-2/b-1*, suggesting that other factors besides JA pathways, such as auxin signaling, are also involved in regulating root growth in the *mob1a-2/b-1* double mutant. This hypothesis is consistent with our previous report that *AtMOB1A* plays a role in auxin-mediated development (Cui et al., 2016). It is likely that *AtMOB1B* plays similar roles in modulating auxin signaling.

Interestingly, it was reported that the expression of *JAZ* genes (*JAZ1*, *JAZ2*, *JAZ5*, *JAZ6*, *JAZ9*, and *JAZ12*) and *MYC* genes (*MYC2*, *MYC3*, and *MYC4*) was repressed in the *sik1* mutant (Xiong et al., 2016), suggesting that *SIK1* also plays roles in JA-related development. However, because the expression of some of the *JAZs* and *MYCs* in the *mob1a-2/b-1* double mutant was up-regulated, it seems that *AtMOB1A/B* and *SIK1* play different roles in modulating JA pathways. Indeed, JA levels were decreased in the *sik1* mutant compared with wild type (Zhang et al., 2018), whereas they were increased in *mob1a-2/b-1* (Fig. 5A). These findings suggest that *SIK1* promotes and *MOB1A/B* represses JA levels. Consistently, the expression levels of *JAZs* and *MYC2* were increased in the *sik1 mob1a-2/b-1* triple mutant compared with in the *sik1*mutant (Fig. 7). It is intriguing how components in the same protein complex would antagonistically modulate JA levels. The *sik1 mob1a-2/b-1* triple-mutant plants showed compromised regulation of JA-related genes, but displayed more severe developmental defects than *sik1* or the *mob1a-2/b-1* double mutant. These results suggest that *MOB1* and *SIK1* may function similarly in controlling cell proliferation, but may have opposite roles in regulating JA levels and JA-related gene expression. The exact molecular mechanisms for such complex regulation are not currently understood. It was reported that the *sik1* mutant exhibited significantly higher levels of basal salicylic acid and decreased levels of JA (Zhang et al., 2018). Since SIK1 plays a role in antibacterial immunity response (Zhang et al., 2018) and MOB1 and SIK1 physically interact, it is possible that MOB1 plays a role in biotic stress responses, perhaps through JA signaling.

AtMOB1A and AtMOB1B Act as Key Regulators in Auxin- and JA-Mediated Plant Growth

Previously, we reported that AtMOB1A plays critical roles in auxin-mediated plant development. We isolated the *mob1a/ncp1* mutant as an enhancer of *pid*, and showed that it had strong genetic interactions with mutants in auxin biosynthesis, polar transport, and signaling (Cui et al., 2016). Disruption of *AtMOB1A* led to a reduced sensitivity to exogenous auxin. Our previous results demonstrated that AtMOB1A plays an important role in Arabidopsis development by promoting auxin signaling (Cui et al., 2016). Our results presented in this paper clearly indicate that AtMOB1A and AtMOB1B also act as key regulators of JA-mediated plant growth. It is likely that AtMOB1A and AtMOB1B physically interact with each other and are components of a large protein complex, which includes SIK1 (Xiong et al., 2016). AtMOB1A and AtMOB1B promote auxin signaling and cell proliferation; however, the two proteins repress JA accumulation. Thus, the AtMOB1-containing protein complex likely regulates the cross talk between auxin- and JA-mediated plant growth and development. A molecular framework for JA-induced inhibition of root growth through interaction with auxin pathways is well established, in which MYC2-mediated repression of PLT expression integrates JA action into the auxin pathway in regulating root meristem activity and stem cell niche maintenance (Chen et al., 2011). Auxin upregulates *PLT1* and *PLT2* transcripts and positively regulates stem cell niche maintenance and meristem activity (Aida et al., 2004), and JA downregulates *PLT1* and *PLT2* expression and negatively regulates stem cell niche maintenance and meristem activity (Chen et al., 2011). We showed that *PLT1/2* expression is repressed in the *mob1a-2/b-1* double mutant, which could be an integrative outcome of elevated JA content and reduced auxin signaling. It would be interesting to further explore the mechanisms by which AtMOB1A/B control JA accumulation and the cross talk with auxin signaling.

MATERIALS AND METHODS

Plant Materials and Growth Condition

All Arabidopsis (*Arabidopsis thaliana*) materials used in this work were in the Col-0 ecotype background. Seeds were surface sterilized for 15 min in 70% (v/v) and then 100% (v/v) ethyl alcohol. The seeds were then sowed on half-strength Murashige and Skoog medium containing 0.8% (w/v) agar. The plates were transferred to 4°C for 3 d in darkness for vernalization. Plants were grown at 22°C under a 16-h light/8-h dark cycle. The T-DNA insertion lines, including *mob1 a-2* (GK_719G04), *mob1 b-1* (SALK_062070), and *mob1 d-1* (SALK_053800), were purchased from the NASC. The *mob1 a-2* (GK_719G04) mutant was genotyped as described previously (Cui et al., 2016). For genotyping *mob1 b-1* (SALK_062070), the primers 5′-GGATGAAGTGTTTGAAGC-3′ and 5′-GCTGAGTAATGG TTGTGA-3′ combined with JMLB1 were used. For genotyping *mob1 d-1* (SALK_053800), the primers 5′-GGGCAAAGTCCAAATCCT-3′ and 5′-CCGCTTCACGAAATCCTC-3′ combined with JMLB1 were used.

DNA Constructs and Plant Transformation

For the expression patterns of *ATMOB1B*, the plasmid was constructed with its genomic DNA fragment containing the coding region alongside up- and down-stream regulatory sequences with the GFP or GUS gene inserted before the stop code. The *AtMOB1B* gene was divided into parts A and B. The part A was amplified using primers 5′-CGGGGTACCGCAGGAATACTATTGGGC CTG-3′ and 5′-ACTGGGCCCGTAAGGTGCAATGATAGATTC-3′. The part B was amplified using primers 5′-ACTGGGCCCACCAAACAAAACCCAAAT CCTC-3′ and 5′-ACTGTCGACGGCTCCAACACAAAATACCTC-3′. The two PCR products were double digested with *KpnI* and *Apa I*, or *ApaI* and *SalI*, respectively, and cloned into the *KpnI-SalI* sites of vector *pPZP211* to generate *pPZP211-gAtMOB1B* construct. The GUS or GFP gene was inserted immediately before the stop code using restriction site of *ApaI*. The *pPZP211-gAtMOB1B-GUS* or *pPZP211-gAtMOB1B-GFP* construct was transformed into *Agrobacterium tumefaciens* strain GV3101, and then Arabidopsis plants were transformed by floral dipping. The transgenic seedlings were selected on half-strength Murashige and Skoog plates with 50 μg/mL kanamycin. The *pPZP211-gAtMOB1A*

(Cui et al., 2016) and *pPZP211-gAtMOB1B-GFP* constructs were used in the complementation experiments of the *mob1a-2/b-1* mutants (Supplemental Fig. S3).

Phenotypic Analysis, Statistical Analysis, and Microscopy

Seedlings and roots were photographed, and their lengths were measured using National Institutes of Health ImageJ software (https://imagej.nih.gov/ij/). Seedlings were mounted in HCG (water-Chloral hydrate-Glycerine) solution (Chloral hydrate:water:glycerol = 8:3:1) and the root meristem cells analyzed on a Leica microsystems DM4500B microscope. Statistical significance was evaluated by Student's *t* test analysis or one-way ANOVA analysis followed by LSD test (SPSS). Histochemical staining for GUS activity in plants was performed as described previously (Cui et al., 2016). For the Lugol staining, roots were incubated in the Lugol solution for 3–5 min, and then washed in water once, and mounted in HCG solution for microscopy analysis. GFP, YFP, CFP, and FM4-64 fluorescence was imaged under a confocal laser scanning microscope Olympus FV1000MPE following the manufacturer's instructions. The fluorescence intensities were measured using ImageJ for quantification analysis.

Co-IP Assays and Mass Spectrometry

For the Co-IP assay of AtMOB1A and AtMOB1B, *pSuper1300:AtMOB1A-Flag* and *pEarleyGate 104-35S:YFP-AtMOB1B* plasmids were constructed and introduced into *Agrobacterium tumefaciens* strain GV3101; then *Nicotiana benthamiana* leaves were transformed by injection. Leaves were ground in liquid nitrogen, and proteins were extracted with same volume of extraction buffer (100 mM HEPES [pH 7.5], 5 mM EDTA, 5 mM EGTA, 10 mM NaF, 5% [v/v] Glycerol, 10 mM Na_3VO_4, 10 mM dithiothreitol, 1 mM phenylmethylsulfonyl fluoride, 0.1% [v/v] Triton X-100, protease inhibitor cocktail [Sigma]). Samples were mixed twice quickly following incubating on ice for 30 min and then centrifuged at 14,000 *g* at 4°C for 30 min. The supernatant was incubated with anti-Flag agarose (Sigma) or Anti-GFP-mAb agarose (MBL) in IP buffer (20 mM Tris-HCl [pH 7.5], 150 mM NaCl, 1 mM EDTA, 1 mM EGTA, 1 mM Na_3VO_4, 1 mM NaF, 10 mM β-glycerophosphate, 0.1% [v/v] Triton X-100, protease inhibitor cocktail [Sigma]) at 4°C for 2 h with gentle shaking. The agarose was collected and washed three times with PBS, boiled in 2×SDS loading buffer for 5 min, and examined by immunoblot analysis with anti-GFP (CWBIO) or anti-Flag (Abmart) antibodies.

For Mass Spectrometry, *pSuper1300:AtMOB1A-Flag* vector was introduced into *Agrobacterium*. Arabidopsis plants were transformed by the floral dipping method. T4 generation transgenic plants were used for extracting total protein and IP using the method described above. The AtMOB1A interacting proteins were examined by Mass Spectrometry.

LCI Assay

The LCI assay was performed as previously described (Chen et al., 2008). *A. tumefaciens* bacteria strain GV3101 containing *pCAMBIA1300-AtMOB1A-nLUC*, *pCAMBIA1300-cLUC-AtMOB1B*, *pCAMBIA1300-nLUC*, and *pCAMBIA1300-cLUC* were injected into *N. benthamiana* leaves. The empty cLUC and nLUC vectors were used as negative controls. The plants were incubated in darkness overnight, and the leaves were harvested after 2 to 3 d. Leaves were incubated in D-Luciferin, Potassium Salt (Goldbio) solution in darkness for 3 min, and the luciferase signals were analyzed with a Tanon 5200 Chemiluminescent Imaging System (Tanon). The imaging exposure time was 3 min. Eight leaves were analyzed for each experiment, with three biological replicates in total.

RNA Extraction, RT-qPCR, and RNA-Seq

The samples were collected from 10-d-old whole seedlings of Col-0, *mob1a-2*, *mob1b-1*, and *mob1a-2 b-1*. Total RNA was extracted using a Biozol kit (Biomiga) according to the manufacturer's instructions. The first-strand complementary DNA synthesis was performed using M-MLV Reverse Transcriptase (Promega). The qPCR analysis was performed using a light cycle 96 (Roche) and SYBR Green I (Takara). *ACTIN2* (*AT3G18780*) was used as an internal control. All experiments were performed with three independent biological replicates. Statistical significance was evaluated by one-way ANOVA analysis (multiple comparison by Tukey post-test). The primers used for RT-qPCR analysis are listed in Supplemental Table S6.

For RNA-seq, mRNA enrichment, complementary DNA library construction, and single-end sequencing were performed by BGI (www.genomics.org.cn). Filtered Clean-reads were mapped to the reference genome (TAIR10) available at The Arabidopsis Information Resource (http://www.arabidopsis.org). The gene expression quantitation was calculated using the RSEM tool (Li and Dewey, 2011). The DEGs were selected according the threshold value fold change ≥2 ($\log_2$ ratio ≥1.0) and deviation probability ≥ 0.7 through comparing the gene expression quantitation of mutants and wild-type. GO enrichment analysis was carried out using AmiGO 2 program (http://amigo.geneontology.org/amigo).

Measurement of Endogenous JA by GC-MS

Fourteen-day-old whole plants of every genotype were collected in triplicate replicates. The samples were homogenized quickly in liquid N_2; then powdered samples were weighed dry-frozen. Samples were extracted with 80% (v/v) methanol containing 0.2 ng [$^2H_6$]JA as an internal standard and incubated overnight at 4°C. After centrifugation at 5,976 *g* for 5 min, the supernatant layer was collected in new glass tubes and dried with nitrogen gas. The samples were dissolved in 2.5% (v/v) ethyl acetate, and the supernatant were dried with nitrogen gas. Following the addition of 23% (v/v) methanol and incubation for 2 h at −20°C, samples were centrifuged at 10,625 *g* for 7 min and the supernatant was dried with nitrogen gas. Samples were dissolved in 30 μL bis(trimethylsilyl) trifluoroacetamide with 3 μL pyridine and incubated for 30 min at 80°C, then analyzed using GC-MS (7890A-7000B, Agilent). The amount of JA present in plant samples was calculated based on the internal standards and weight of the tissues and retention time.

Measurement of Chlorophyll Content

Measurement of chlorophyll content was performed as previously described (Qi et al., 2015). The leaves were detached and weighted. For chlorophyll extraction, the leaves were incubated in 80% (v/v) acetone in the dark. Absorbances were measured at 645 and 663 nm using a spectrophotometer (Beckman Coulter DU-800). Chlorophyll contents were calculated and expressed as a ratio of the chlorophyll content of Col-0 treated with mock.

Accession Numbers

Sequence data from this article can be found in the GenBank/EMBL data libraries under accession numbers JAZ1 (AT1G19180), JAZ2 (AT1G74950), JAZ3 (AT3G17860), JAZ4 (AT1G48500), JAZ5 (AT1G17380), JAZ6 (AT1G72450), JAZ7 (AT2G34600), JAZ8 (AT1G30135), JAZ9 (AT1G70700), JAZ10 (AT5G13220), JAZ11 (AT3G43440), and JAZ12 (AT5G20900).

Supplemental Data

The following supplemental materials are available.

Supplemental Figure S1. Analysis of T-DNA insertion lines of AtMOB1 genes and generation of CRISPR line of AtMOB1C.

Supplemental Figure S2. Representative images of 21-d-old plants of Col-0, *mob1a-2*, *mob1b-1*, and *mob1a-2/b-1* mutants.

Supplemental Figure S3. Complementation of *mob1a-2/b-1* with a genomic DNA fragment of *AtMOB1A* or *AtMOB1B*.

Supplemental Figure S4. Expression patterns of *AtMOB1A* and *AtMOB1B* and subcellular localization of the proteins.

Supplemental Figure S5. JA treatment of seedlings at different concentrations.

Supplemental Figure S6. *pWOX5:GFP* expression in the root of 6-d-old seedlings.

Supplemental Table S1. MOB1B was identified by IP-MS assays in MOB1A-Flag transgenic plants.

Supplemental Table S2. List of differentially expressed genes (DEGs).

Supplemental Table S3. Enriched GO categories in biological process of the DEGs.

Supplemental Table S4. DEGs involved in JA related pathway.

Supplemental Table S5. DEGs involved in leaf senescence.

Supplemental Table S6. Primers used for RT-qPCR reactions.

ACKNOWLEDGMENTS

We thank Dr. Yunde Zhao for critical reading of the manuscript, Dr. Daoxin Xie and Dr. Susheng Song for providing the *myc2* mutant seeds, Dr. Qingqiu Gong for *sik1* mutant seeds, Dr. Yuxin Hu for the Chemiluminescent Imaging System, Dr. Jianmin Zhou for the LCI system vectors, and Dr. Li-jia Qu for insightful discussion. We thank Lu Wang and Jingquan Li for their excellent technical assistance, and the Plant Science Facility of the Institute of Botany, Chinese Academy of Sciences.

Received November 15, 2019; accepted December 4, 2019; published December 20, 2019.

LITERATURE CITED

Aida M, Beis D, Heidstra R, Willemsen V, Blilou I, Galinha C, Nussaume L, Noh YS, Amasino R, Scheres B (2004) The PLETHORA genes mediate patterning of the Arabidopsis root stem cell niche. Cell **119:** 109–120

Chen H, Zou Y, Shang Y, Lin H, Wang Y, Cai R, Tang X, Zhou JM (2008) Firefly luciferase complementation imaging assay for protein-protein interactions in plants. Plant Physiol **146:** 368–376

Chen Q, Sun J, Zhai Q, Zhou W, Qi L, Xu L, Wang B, Chen R, Jiang H, Qi J, et al (2011) The basic helix-loop-helix transcription factor MYC2 directly represses PLETHORA expression during jasmonate-mediated modulation of the root stem cell niche in Arabidopsis. Plant Cell **23:** 3335–3352

Chow A, Hao Y, Yang X (2010) Molecular characterization of human homologs of yeast MOB1. Int J Cancer **126:** 2079–2089

Citterio S, Piatti S, Albertini E, Aina R, Varotto S, Barcaccia G (2006) Alfalfa Mob1-like proteins are involved in cell proliferation and are localized in the cell division plane during cytokinesis. Exp Cell Res **312:** 1050–1064

Colón-Carmona A, You R, Haimovitch-Gal T, Doerner P (1999) Technical advance: Spatio-temporal analysis of mitotic activity with a labile cyclin-GUS fusion protein. Plant J **20:** 503–508

Cui X, Guo Z, Song L, Wang Y, Cheng Y (2016) NCP1/AtMOB1A plays key roles in auxin-mediated Arabidopsis development. PLoS Genet **12:** e1005923

Galinha C, Hofhuis H, Luijten M, Willemsen V, Blilou I, Heidstra R, Scheres B (2007) PLETHORA proteins as dose-dependent master regulators of Arabidopsis root development. Nature **449:** 1053–1057

Galla G, Zenoni S, Marconi G, Marino G, Botton A, Pinosa F, Citterio S, Ruperti B, Palme K, Albertini E, et al (2011) Sporophytic and gametophytic functions of the cell cycle-associated Mob1 gene in *Arabidopsis thaliana* L. Gene **484:** 1–12

Gao X, Chen J, Dai X, Zhang D, Zhao Y (2016) An effective strategy for reliably isolating heritable and Cas9-free Arabidopsis mutants generated by CRISPR/Cas9-mediated genome editing. Plant Physiol **171:** 1794–1800

Goto H, Nishio M, To Y, Oishi T, Miyachi Y, Maehama T, Nishina H, Akiyama H, Mak TW, Makii Y, et al (2018) Loss of *Mob1a/b* in mice results in chondrodysplasia due to YAP1/TAZ-TEAD-dependent repression of SOX9. Development **145:** dev159244

Hansen CG, Moroishi T, Guan KL (2015) YAP and TAZ: A nexus for Hippo signaling and beyond. Trends Cell Biol **25:** 499–513

Harvey KF, Zhang X, Thomas DM (2013) The Hippo pathway and human cancer. Nat Rev Cancer **13:** 246–257

He Y, Fukushige H, Hildebrand DF, Gan S (2002) Evidence supporting a role of jasmonic acid in Arabidopsis leaf senescence. Plant Physiol **128:** 876–884

Huang H, Liu B, Liu L, Song S (2017) Jasmonate action in plant growth and development. J Exp Bot **68:** 1349–1359

Lai ZC, Wei X, Shimizu T, Ramos E, Rohrbaugh M, Nikolaidis N, Ho LL, Li Y (2005) Control of cell proliferation and apoptosis by mob as tumor suppressor, mats. Cell **120:** 675–685

Li B, Dewey CN (2011) RSEM: Accurate transcript quantification from RNA-Seq data with or without a reference genome. BMC Bioinformatics **12:** 323

Lorenzo O, Chico JM, Sánchez-Serrano JJ, Solano R (2004) JASMONATE-INSENSITIVE1 encodes a MYC transcription factor essential to discriminate between different jasmonate-regulated defense responses in Arabidopsis. Plant Cell **16:** 1938–1950

Luca FC, Winey M (1998) MOB1, an essential yeast gene required for completion of mitosis and maintenance of ploidy. Mol Biol Cell **9:** 29–46

Nishio M, Hamada K, Kawahara K, Sasaki M, Noguchi F, Chiba S, Mizuno K, Suzuki SO, Dong Y, Tokuda M, et al (2012) Cancer susceptibility and embryonic lethality in Mob1a/1b double-mutant mice. J Clin Invest **122:** 4505–4518

Nishio M, Sugimachi K, Goto H, Wang J, Morikawa T, Miyachi Y, Takano Y, Hikasa H, Itoh T, Suzuki SO, et al (2016) Dysregulated YAP1/TAZ and TGF-β signaling mediate hepatocarcinogenesis in Mob1a/1b-deficient mice. Proc Natl Acad Sci USA **113:** E71–E80

Pan D (2010) The hippo signaling pathway in development and cancer. Dev Cell **19:** 491–505

Pinosa F, Begheldo M, Pasternak T, Zermiani M, Paponov IA, Dovzhenko A, Barcaccia G, Ruperti B, Palme K (2013) The *Arabidopsis thaliana* Mob1A gene is required for organ growth and correct tissue patterning of the root tip. Ann Bot **112:** 1803–1814

Qi T, Wang J, Huang H, Liu B, Gao H, Liu Y, Song S, Xie D (2015) Regulation of jasmonate-induced leaf senescence by antagonism between bHLH subgroup IIIe and IIId factors in Arabidopsis. Plant Cell **27:** 1634–1649

Shan X, Wang J, Chua L, Jiang D, Peng W, Xie D (2011) The role of Arabidopsis Rubisco activase in jasmonate-induced leaf senescence. Plant Physiol **155:** 751–764

Titarenko E, Rojo E, León J, Sánchez-Serrano JJ (1997) Jasmonic acid-dependent and -independent signaling pathways control wound-induced gene activation in *Arabidopsis thaliana*. Plant Physiol **115:** 817–826

Vitulo N, Vezzi A, Galla G, Citterio S, Marino G, Ruperti B, Zermiani M, Albertini E, Valle G, Barcaccia G (2007) Characterization and evolution of the cell cycle-associated mob domain-containing proteins in eukaryotes. Evol Bioinform Online **3:** 121–158

Wang W, Li X, Huang J, Feng L, Dolinta KG, Chen J (2014) Defining the protein-protein interaction network of the human hippo pathway. Mol Cell Proteomics **13:** 119–131

Wasternack C, Song S (2017) Jasmonates: Biosynthesis, metabolism, and signaling by proteins activating and repressing transcription. J Exp Bot **68:** 1303–1321

Xiao S, Dai L, Liu F, Wang Z, Peng W, Xie D (2004) COS1: An Arabidopsis coronatine insensitive1 suppressor essential for regulation of jasmonate-mediated plant defense and senescence. Plant Cell **16:** 1132–1142

Xiong J, Cui X, Yuan X, Yu X, Sun J, Gong Q (2016) The Hippo/STE20 homolog SIK1 interacts with MOB1 to regulate cell proliferation and cell expansion in Arabidopsis. J Exp Bot **67:** 1461–1475

Zeng W, Dai X, Sun J, Hou Y, Ma X, Cao X, Zhao Y, Cheng Y (2018) Modulation of auxin signaling and development by polyadenylation machinery. Plant Physiol **179:** 686–699

Zhang M, Chiang YH, Toruno TY, Lee D, Ma M, Liang X, Lal NK, Lemos M, Lu YJ, Ma S, et al (2018) The MAP4 kinase SIK1 ensures robust extracellular ROS burst and antibacterial immunity in plants. Cell Host Microbe **24:** 379–391